JOURNAL OF MATERIALS SCIENCE 26 (1991) 2527–2532

Effect of surface treatment on segregation of impurities in haematite

A. BERNASIK, J. JANOWSKI
Institute of Metallurgy, Academy of Mining and Metallurgy, 30-059 Krakow, Poland
W. HIRSCHWALD, F. STOLZE
Free University of Berlin, Institute of Physical Chemistry, W-1000 Berlin 33, FRG
J. NOWOTNY*
Max-Planck-Institute for Solid State Research, W-7000 Stuttgart 80, FRG

Surface segregation of various impurities such as Mg, Si, Ca, Al and Cr were determined for the haematite phase (Fe_2O_3) annealed in two different gas compositions involving (1) air at 1173 K, and (2) a gas mixture containing sulphur at 773 K. The objective of work was to establish the effect of the gas-phase composition on segregation of lattice defects. The near-surface segregation profiles of the impurities were determined by secondary ion mass spectrometry. The depth profile analysis was made by sputtering using an Ar^+ primary beam of energy 30 keV. The surface charge was neutralized by an electron gun. It was found that annealing Fe_2O_3 under a gas phase containing sulphur resulted in the formation of an $Fe(SO_4)_3$ surface layer. It was observed that the two surface treatment procedures applied (both with and without sulphur) result in Mg enrichment in the near-surface region of Fe_2O_3. Si and Ca exhibit an enrichment and impoverishment after the surface treatments 1 and 2, respectively. Finally, the near-surface layer is impoverished in Cr and Al after both types of surface treatment. Experimental results are discussed in terms of segregation driving forces of the respective elements and the possible effect of sulphur on the gas–solid heterogeneous kinetics.

---

1. Introduction

Lattice defects, such as intrinsic lattice defects and foreign elements segregate to interfaces of solids leading to the formation of concentration gradients within the interface region [1–4]. In certain cases segregation results in structural deformations of the outer surface layer and the formation of low-dimensional interface structures of extraordinary properties [3, 4]. The interface layer formed as a result of segregation may have a substantial effect on many properties of materials, especially of ceramics. Therefore, interest was generated in studies of surface and grain-boundary segregation in solids [5–8].

For a long time the research on segregation was oriented towards metals and alloys [5, 6, 9]. In contrast to metals, the surface studies of ionic solids are more difficult, because of charging effects accompanying bombardment of the surface. Also the preparation of a well-defined surface of the compounds is the subject of substantial difficulties. The interest in surface studies of ionic solids was generated after it was observed that interfaces such as external surfaces and grain boundaries have a substantial effect on processes and properties of ceramic materials. A very spectacular phenomenon involves the effect of Mg segregation on the mechanism and kinetics of sintering of alumina, leading to the formation of high-density material [10–12].

The extent of segregation depends on many parameters, such as mismatch between host ions and segregating species, temperature and chemical composition of the bulk phase and the gas phase [1–4]. The relation between the bulk-phase composition and the interface composition of solids is given by the Gibbs' equation

$$\Gamma_i = -\frac{1}{RT}\left(\frac{\partial\gamma}{\partial \ln a_i}\right)_{T,a_j} \qquad (1)$$

where Γ_i denotes the surface excess number, a_i is the chemical activity of the ith element, γ is the surface tension and R and T have their traditional meaning. Equation 1 has been verified for metallic systems and it should essentially be valid also for ionic solids.

The composition of the gas phase has an effect on the composition of the bulk phase as a result of interactions between the two phases. The effect is especially pronounced at elevated temperatures. In the case of metal-deficient oxides ($M_{1-y}O$) the following relationship can be written between the deviation from stoichiometry (y) and oxygen activity in the gas phase

$$y = \text{const}\, p_{O_2}^{1/n} \qquad (2)$$

where n is a parameter. Equation 2 is valid when equilibrium between the gas phase and the solid phase

---

*Present address: Australian Nuclear Science and Technology Organisation, Menai, NSW 2234, Australia.

0022–2461/91 $03.00 + .12 © *1991 Chapman and Hall Ltd.*

is reached. Thus one may expect that p_{O_2} and the resulting oxide non-stoichiometry will have an effect on the extent of segregation. The effect has been confirmed experimentally for Cr segregation in NiO [13], CoO [14] and MgO [15]. The objective of this work was to study the effect of the gas-phase composition on the cation segregation in Fe_2O_3.

Haematite is an important material in metallurgy. It has been reported that the reduction kinetics of this material depends on the presence of sulphur in the gas phase [16–18]. This effect, which has been observed already at the level of 50 p.p.m. of sulphur, is not well understood [16]. A possible approach to the study of this effect should involve a superficial microchemical analysis of Fe_2O_3 after thermal treatment in a sulphur-containing atmosphere in order to evaluate the effect of sulphur in the gas phase on surface composition. Therefore, in the present work studies of near-surface concentration profiles of lattice elements of Fe_2O_3 were performed after different standardization procedures involving the surface treatment in a gas phase free of sulphur as well as sulphur-containing gas atmospheres. Secondary ion mass spectrometry (SIMS) was used as the main technique, in addition to X-ray photoelectron spectroscopy (XPS).

2. Secondary ion mass spectrometry of metal oxides – general consideration

Surface bombardment by a primary ion beam results in the emission of the secondary beam composed of ions and clusters of different effective charge. The current of secondary ions can be expressed by the following formula

$$I_M = I_R f_M S_M \alpha_M^+ C_M \tag{3}$$

where I_R denotes the current of primary ions, f_M the transmission factor, C_M the concentration of element M, S_M the sputtering coefficient, and α_M^+ the ionization probability. For determination of the concentration parameter, C_M, it is necessary to perform a calibration procedure and the determination of parameters f_M and S_M^+, where S_M^+ is the ion sputter yield given by

$$S_M^+ = S_M \alpha_M^+ \tag{4}$$

Chemical composition of the secondary beam may differ from that of the analysed surface spot. In the case of metal oxides, the oxygen sputter ion yield is much larger than that of the metal. This results in a reduction of the surface [19–22] which may lead to changes in parameters S_M and S_M^+. Accordingly, in the case of compounds, calibration studies are required for a correct determination of the interrelationship between concentrations of lattice ions and intensity values.

In many cases, experimental data on near-surface concentration profiles are reported in the form of relative intensity ratios of elements. These data enable evaluation the segregation tendency to be made qualitatively. Experimental data in the present work will also be reported in this form.

3. Experimental procedure

A polycrystalline sample of Fe_2O_3 was prepared by sintering of a spectrally pure powder. Sintering was performed at 1673 K in air for 10 h. The sample was used in the form of a pellet. The following major, unintentional contaminations were present in the specimen: $SiO_2 < 0.005\%$, $Ni < 0.002\%$, $Mn < 0.005\%$, $Mg < 0.03\%$, $Ca < 0.05\%$ and $Zn < 0.005$.

The sample was the subject of standardization procedures involving the thermal treatments under two different atmospheres. The treatments involved (1) heating in air for 17 h at 1273 K (oxygen standardization), (2) heating for 1 h at 773 K under a gas mixture of composition 0.9 atm N_2 (sulphur standardization) and 0.1 atm H_2S. The oxygen partial pressure in nitrogen was about 0.001 atm.

The near-surface concentration profiles were determined by using the SIMS facility of VG ESCALAB 5 equipment. The sputtering was performed using a primary Ar^+ beam of 3 keV. Two sputtering procedures were applied. The first (procedure I) involved a current ion density of 1.1 $\mu A\,cm^{-2}$ with the target dimension 0.7 mm^2. The second procedure (procedure II) involved 15 $\mu A\,cm^{-2}$. The target area of all specimens studied was 24 mm^2. Assuming the sputter yield $s = 1$, these sputtering procedures correspond to about 0.2 and 2.8 $nm\,min^{-1}$ erossion rate, respectively. An electron gun was applied to neutralize the surface charge.

The XPS studies were performed by using AlK_α radiation of energy 1486.6 eV. Energy calibration was performed with reference to the main peak O 1s of binding energy 530 eV. According to the literature [19, 21, 23, 24] its position for different iron oxides remains constant within 0.1 eV.

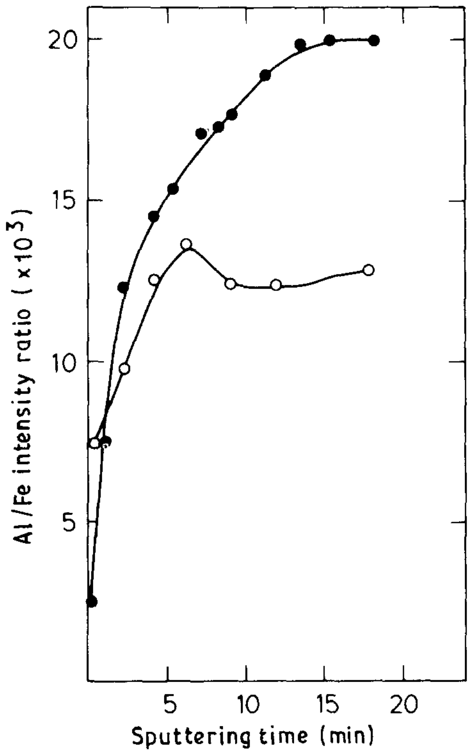

Figure 1 Al/Fe intensity ratios versus sputtering time (procedure I). (○) Oxygen standardization, (●) sulphur standardization.

4. Results

Qualitative SIMS analyses have indicated the following major impurities in the outer surface layer of the studied Fe_2O_3 specimen: Al, Ca, Si, Mg and Cr. Figs 1–5 illustrate the near-surface concentration profiles of these elements plotted in the form of the relative intensity ratios versus the time of sputtering, using sputtering procedure I. As seen, the surface treatment under both gas atmospheres results in a Mg-enrichment of the outer oxide layer (Fig. 4). The reverse effect is observed in the case of Al and Cr (Fig. 1 and 5, respectively). The effect is more complicated in the case of both Ca and Si. For these two elements the treatment in oxygen and sulphur results in an enrichment and impoverishment, respectively. These effects were independent of the sputtering rate and the sputtering geometry. As seen from Figs 6–9, the same phenomena are observed for both sputtering procedures.

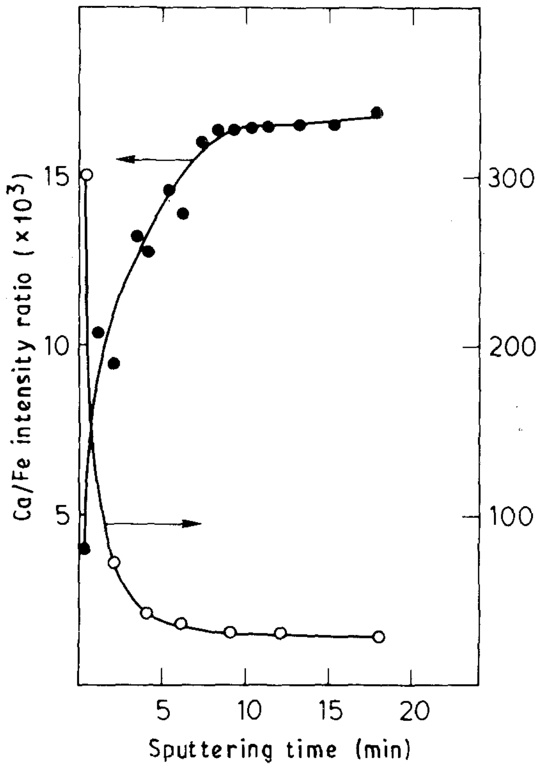

Figure 2 Ca/Fe intensity ratios versus sputtering time (procedure I). For key, see Fig. 1.

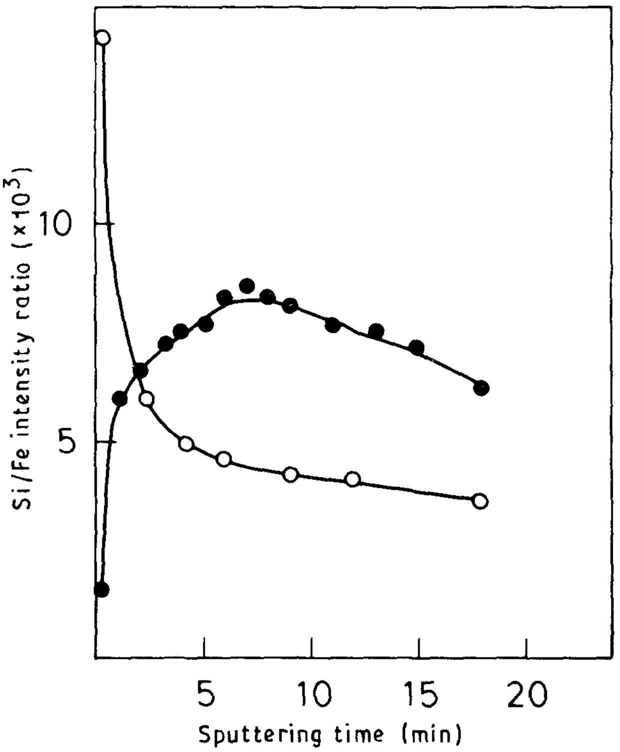

Figure 3 Si/Fe intensity ratios versus sputtering time (procedure I). For key, see Fig. 1.

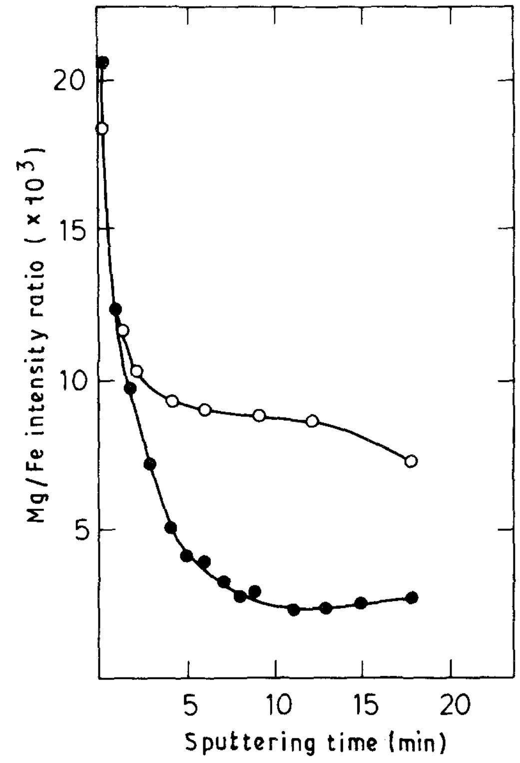

Figure 4 Mg/Fe intensity ratios versus sputtering time (procedure I). For key, see Fig. 1.

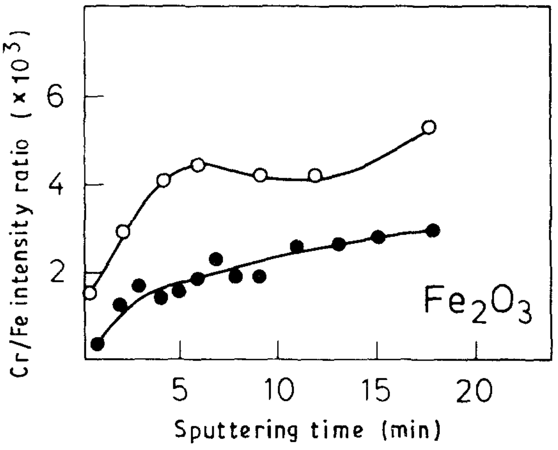

Figure 5 Cr/Fe intensity ratios versus sputtering time (procedure I). For key, see Fig. 1.

The binding energies determined by XPS are listed in Table I.

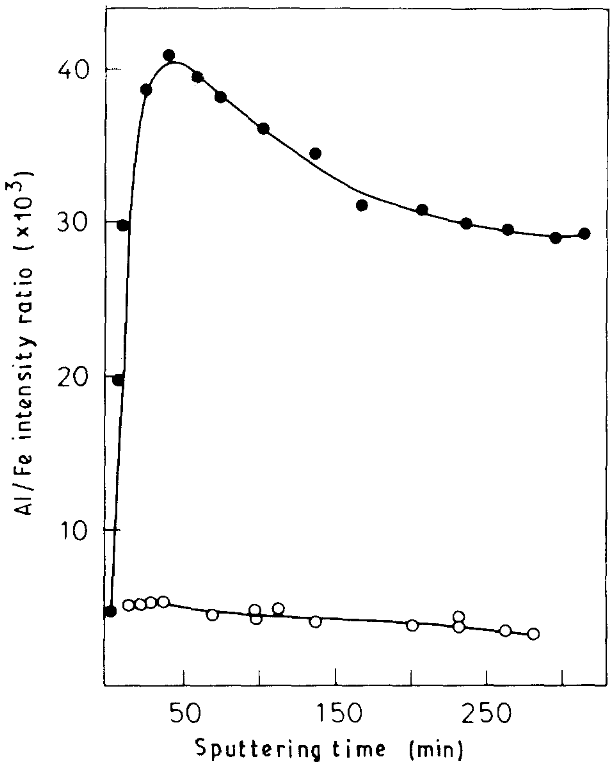

Figure 6 Al/Fe intensity ratios versus sputtering time (procedure II). For key, see Fig. 1.

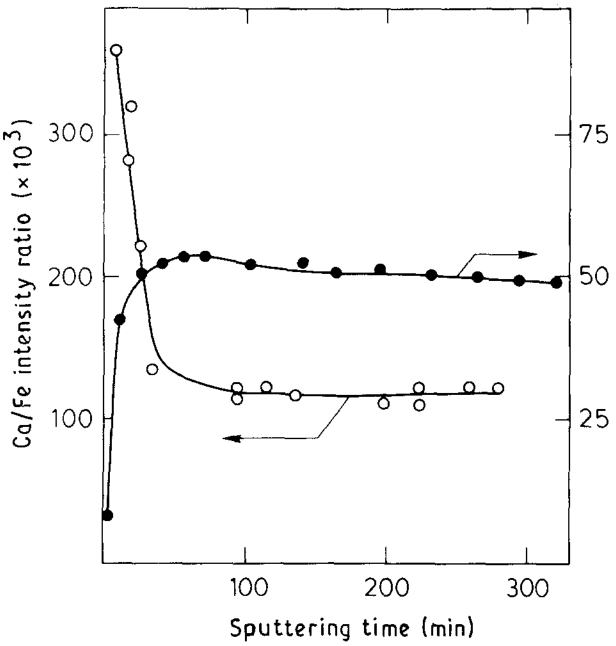

Figure 7 Ca/Fe intensity ratios versus sputtering time (procedure II). For key, see Fig. 1.

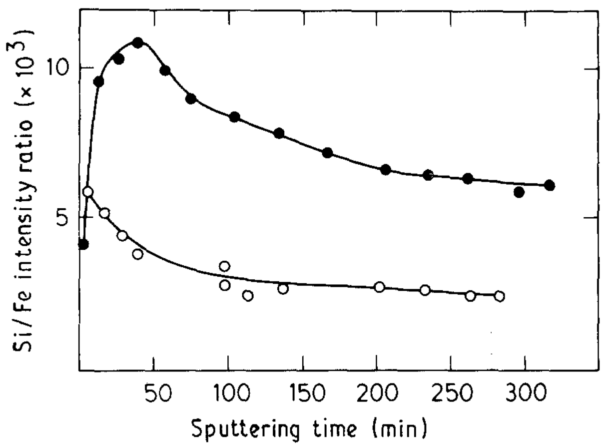

Figure 8 Si/Fe intensity ratios versus sputtering time (procedure II). For key, see Fig. 1.

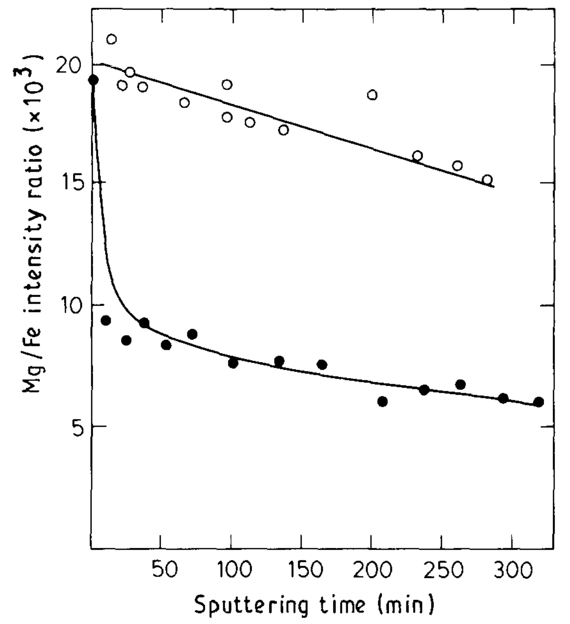

Figure 9 Mg/Fe intensity ratios versus sputtering time (procedure II). For key, see Fig. 1.

5. Discussion

Comparison of the obtained experimental data with ionic radii of the host lattice ion (Fe^{3+}) and segregating ions indicates that the fundamental segregation driving force is related to the decrease in the lattice strength energy as a result of ionic mismatch. Table II gives values of the ionic radii for cations considered in this work. Mg segregation cannot be explained in terms of the decrease in the strength energy because the mismatch between Mg^{2+} and Fe^{3+} ions is negative. Apparently, the electrostatic term, resulting from the charge difference of both ions, results in Mg segregation in both gas atmospheres. On the other hand, an impoverishment in Al for both standardization procedures is consistent with a negative mismatch between Al^{3+} and Fe^{3+} ions. Therefore, the observed positive and negative segregation tendency of these two ions is in accordance with the tendency to reduce the lattice strain energy. The positive mismatch between Fe^{3+} and Cr^{3+} ions suggests that the surface will be enriched in Cr. The observed impoverishment under both gas compositions indicates that this segregation driving force is not the prevailing one. Also the electrostatic approach cannot be considered in this case. Therefore a possible explanation of Cr segregation in Fe_2O_3 may involve the formation of an overlayer low-energy structure.

For both Ca and Si the two applied standardization procedures lead to a different picture of depth profiles. The observed enrichment in Ca for the sample standardized in air is in agreement with the strain energy

TABLE I Binding energies of the Fe_2O_3 specimen

Sputtering time (procedure II) (min)	Standardization	Fe $2p_{3/2}$ (eV)	Fe $2p_{1/2}$ (eV)	S 2p (eV)
0	Oxygen	710.9 ± 0.3	729.5 ± 0.3	
2	Oxygen	710.9 ± 0.3	723.6 ± 0.3	
6	Oxygen	710.2 ± 0.3	723.3 ± 0.3	
10	Oxygen	710.3 ± 0.3	723.3 ± 0.3	
0	Sulphur	710.9 ± 0.3	724.5 ± 0.3	168.8 ± 0.4
2	Sulphur	710.7 ± 0.3	723.9 ± 0.3	ND
6	Sulphur	710.1 ± 0.3	723.2 ± 0.3	ND
10	Sulphur	710.1 ± 0.3	723.2 ± 0.3	ND

ND – not detected

TABLE II Ionic radii of both host lattice cations and impurities

Ion	Fe^{3+}	Fe^{2+}	Al^{3+}	Mg^{2+}	Ca^{2+}	Si^{4+}	Cr^{3+}
Radius (pm)	64	76	0.5	65	100	41	69

model. The impoverishment (negative segregation) of the surface layer in Ca after sulphur annealing indicates that the predominant driving force in this case is different. Apparently, the formation of the two-dimensional overlayer structure is responsible for a change in the sign of the segregation driving force. Similarly, the size mismatch between Si and Fe ions is in agreement with the depletion of Si in the surface layer after sulphur standardization, but the reverse effect, observed after oxygen standardization, is not clear. These results are essentially confirmed by experimental data obtained by sputtering procedure II (Figs 6–9).

XPS studies indicate that the binding energy of the sulphur 2p level for the specimen standardized in sulphur coincides well with that for $Fe_2(SO_4)_3$. Accordingly, one may conclude that the gas composition containing sulphur favours the formation of a low-dimensional layer of $Fe_2(SO_4)_3$. One may expect that the formation of different structures under both standardization procedures are responsible for the different sign of segregation observed for both Ca and Si (positive and negative segregation after procedures 1 and 2, respectively).

The observed shift of the $2p_{3/2}$ level of iron towards lower binding-energy values (Table I) indicates that sputtering results in reduction of the analysed surface spot. The reduction, however, does not lead to the formation of the metallic phase, as reported by Brundle *et al.* [21].

6. Conclusions

Studies of chemical composition of the near-surface regions of the haematite phase (Fe_2O_3) have shown the presence of several contaminations. The contaminations, which are present in the bulk at a low level of several tenths and hundreths of p.p.m., lead to an enrichment of the surface as a result of segregation. The depth profile analysis has shown that the near-surface composition strongly depends on the composition of the gas phase during the thermal pretreatment. In certain cases an impoverishment of the surface layer can be observed.

Sulphur present in the gas phase may interact with the outer surface layer leading to the formation of superficial structures or low-dimensional surface phases. These phases and the Schottky-type barrier resulting from the heterogeneous junction thus formed may have a strong effect on the transport kinetics of charged defects across this barrier. Consequently, one may expect that the barrier formed during the segregation may have an effect on the entire gas–solid heterogeneous kinetics during the reduction of haematite, as observed by Adam *et al.* [16–18].

The observed enrichment of the surface in Si after oxygen standardization cannot be explained by the strain–energy term. The explanation of Si segregation in oxygen may be related to the formation of the surface two-dimensional phase, as reported by Ettabirou *et al.* [25].

References

1. P. WYNBLATT and R. C. McCUNE, in "Surface and Near-Surface Chemistry of Oxide Materials", edited by J. Nowotny and L. C. Dufour (Elsevier, Amsterdam, 1988) p. 247.
2. A. J. BURGGRAAF and A. J. A. WINNUBST, *ibid.*, p. 449.
3. J. NOWOTNY, *Solid State Ionics* **28–30** (1988) 1243.
4. *Idem.*, *Mater. Sci. Forum* **29** (1988) 99.
5. C. LEYGRAF, S. EKELUND and G. SCHÖN, *Scand. J. Metall.* **2** (1973) 313.
6. F. J. KUIJERS and V. PONEC, *Surf. Sci.* **68** (1977) 294.
7. W. C. MACKRODT and P. W. TASKER, *Chemistry in Britain*, April (1985) 366.
8. D.W. KINGERY, *J. Amer. Ceram. Soc.* **57** (1974) 1.
9. C. LEYGRAF, G. HULTQUIST, S. EKELUND and J. C. ERIKSSON, *Surf. Sci.* **46** (1974) 157.
10. R. I. TAYLOR, J. P. COAD and R. J. BROOK, *J. Amer. Ceram. Soc.* **57** (1974) 539.
11. S. BAIK, *ibid.* **68** (1985) 281.
12. S. BAIK and C. L. WHITE, *ibid.* **70** (1987) 682.
13. W. HIRSCHWALD, I. SIKORA and F. STOLZE, *Surf. Interface Anal.* **3** (1985) 157.
14. I. SIKORA, F. STOLZE and W. HIRSCHWALD, *ibid.* **10** (1987) 424.
15. J. R. H. BLACK and W. D. KINGERY, *J. Amer. Ceram. Soc.* **62** (1979) 176.
16. F. ADAM, These d'Etat, Université de Nancy, Nancy (1988).
17. F. ADAM, B. DUPRÉ and C. GLEITZER, *Mem. Etudes Sci. Rev. Metall.*, in press.
18. F. ADAM, F. JEANNOT, B. DUPRÉ and C. GLEITZER, *React. Solids* **5** (1988) 115.
19. E. PAPARAZZO, *Surf. Interface Anal.* **12** (1988) 115.

20. G. PANZNER, B. EGERT and H. P. SCHMIDT, *ibid.* (1985) 400.
21. C. R. BRUNDLE, T. J. CHUANG and K. WANDELT, *Surf. Sci.* **68** (1977) 459.
22. T. J. CHUANG, C. R. BRUNDLE and D. W. RICE, *ibid.* **59** (1976) 413.
23. N. S. McINTYRE and D. G. ZETARUK, *Anal. Chem.* **49** (1977) 1521.
24. G. C. ALLEN, M. T. CURTIS, A. J. HOOPER and P. M. TUCKER, *J. Chem. Soc. Dalton Trans.* **14** (1974) 1525.
25. M. ETTABIROU, B. DUPRÉ and Ch. GLEITZER, *Steel Res.* **57** (1986) 306.

Received 8 January
and accepted 14 August 1990